

Title: *Haloquadratum walsbyi* yields a versatile, NAD^+ / $NADP^+$ dual affinity, thermostable, alcohol dehydrogenase (HwADH)

Authors: Jennifer Cassidy^{a,b} and Francesca Paradisi^{a,b*}

^a *School of Chemistry, University Park, University of Nottingham, NG7 2RD, UK*

^b *Synthesis and Solid State Pharmaceutical Centre (SSPC), School of Chemistry, University College Dublin, Belfield, Dublin 4, Ireland*

Electronic supplementary information (ESI) available:

*Corresponding author

Francesca Paradisi

E-mail: Francesca.Paradisi@nottingham.ac.uk

Telephone: +44-115-74 86267

Address: School of Chemistry, University Park, University of Nottingham, NG7 2RD, UK

Abbreviations

ACN; acetonitrile, ADH; alcohol dehydrogenase, IMAC; immobilised metal-affinity chromatography, iPrOH: isopropanol, SDS-PAGE; sodium dodecyl sulfate polyacrylamide gel electrophoresis, EtOH; ethanol, BzOH; benzyl alcohol, CycOH; cyclohexanol, 1-PheOH; 1-phenylethanol, (*S*)-1-PheOH; (*S*)-1-phenylethanol, (*R*)-1-PheOH; (*R*)-1-phenylethanol, 2-Phe-1-Prop; 2-phenyl-1-propanol

Keywords: *Haloquadratum walsbyi*, alcohol dehydrogenase, thermoactivity, dual cofactor specificity

Abstract

This study presents the first example of an alcohol dehydrogenase (ADH) from the halophilic archaeum *Haloquadratum walsbyi* (*HwADH*). A hexahistidine-tagged recombinant *HwADH* was heterologously overexpressed in *Haloferax volcanii*. *HwADH* was purified in one step and was found to be thermophilic with optimal activity at 65 °C. *HwADH* was active in the presence of 10 % (v/v) organic solvent. The enzyme displayed dual cofactor specificity and a broad substrate scope, maximum activity was detected with benzyl alcohol and 2-phenyl-1-propanol. *HwADH* accepted aromatic ketones, acetophenone and phenylacetone as substrates. The enzyme also accepted cyclohexanol and aromatic secondary alcohols, 1-phenylethanol and 4-phenyl-2-butanol. *H. walsbyi* may offer an excellent alternative to other archaeal sources to expand the toolbox of halophilic biocatalysts.

Introduction

Haloquadratum walsbyi are flat, square cells, most recognisable as having postage-stamp shape; their characteristic gas vacuoles afford buoyancy in salt lakes (Stoeckenius 1981; Walsby 1980). Compared to other members of *Halobacteriaceae*, *Haloquadratum walsbyi* have an unusually low GC content (47.9%) (Bolhuis et al. 2006) which effects the third codon, at the nucleotide. However, many of the proteins encoded by *H. walsbyi* presents similar characteristics to other halophilic proteins with a high percentage of acidic residues (average pI = 5.1) (Bolhuis et al. 2006). *Haloquadratum walsbyi* follow the same “salt-in” strategy as other Halobacteriaceae by maintaining a high concentrations of inorganic ions in the cytoplasm. Typically, K⁺ is the preferred cation, and Cl is the dominant anion (Becker et al. 2014). The similar GC content of *E. coli* (51 %) would imply that expression of a protein from *Haloquadratum walsbyi* could also be attempted in a mesophilic host.

Despite their biodiversity and prevalence in hypersaline waters around the world, it took 25 years to obtain a pure culture *Haloquadratum walsbyi* (Burns et al. 2004). Hence, examples of homologous or heterologous expression of *Haloquadratum* proteins have been sparse in the literature. This is in stark contrast to the plethora of knowledge and molecular tools available for *Haloferax volcanii* (Allers et al. 2010; Hartman et al. 2010; Large et al. 2007). Three proteins from *Haloquadratum walsbyi*, a halorodhopsin, a rhodopsin, and a alpha-glucosidase were successfully cloned, expressed and solubilized from *E. coli* (Fu et al. 2012; Sudo et al. 2011; Cuebas-Irizarry et al. 2017), proving the ability of *E. coli* to express proteins

from this archaeon without need for gene optimisation. In another example, a computational protein design approach was used to develop a stable biocatalyst variant from *Haloquadratum walsbyi* DSM 16790, but this remained an *in silico* design (Chellapandi and Balachandramohan 2011).

The enzymes from halophilic archaea have novel activities that are distinct from their mesophilic equivalents. Halophiles have become interesting industrial catalysis candidates due to their adaptations in low water activity. This means that they are active in some organic solvents, which may be advantageous industrially, due to increased solubility of non-polar substrates (Sellek and Chaudhuri 1999; Yu and Li 2014). Some industrial applications of halophiles and halo-adapted organisms include the production of β -carotene by *Dunaliella salina* (Borowitzka and Siva 2007), and the production of ectoine (1,4,5,6-tetrahydro-2-methyl-4-pyrimidinecarboxylic acid) by *Halomonas elongata* and *Marinococcus* M52 (Oren 2002b). β -carotene is used as an antioxidant and as a food colouring agent (Oren 2002a), while ectoine is used as an enzyme stabiliser and is also used in moisturizers in cosmetics, *Dunaliella* cell biomass is also used in “anti-wrinkle” cosmetics (Oren 2002b).

Alcohol dehydrogenases (ADHs) can reduce pro-chiral ketones to optically active secondary alcohols, highly desirable intermediates for the pharmaceutical industry. The first example of a halophilic ADH (*NpADH*), was mined from the genome of *Natronomonas pharaonis*, expressed in *E. coli* and found to be alkaliphilic, thermoactive and extremely salt-dependent (Cao et al. 2008). Within our lab we have fully characterised several halophilic ADHs. *HmADH12* (*Haloarcula marismortui*) was heterologously overexpressed and purified from *Haloferax volcanii* (Timpson et al. 2012). Characterisation of this biocatalyst ignited our search

for more halophilic ADHs. *HsADH2* from the extremely halophilic archaeon *Hbt. sp. NRC-1*, was identified but initial expression yielded very little protein. Again, expression in *Haloferax volcanii* facilitated overexpression and purification of *HsADH2*. *HsADH2* was extremely stable, showed dual cofactor specificity and displayed intrinsic organic solvent tolerance (Liliensiek et al. 2013). Two ADHs from *Haloferax volcanii*, *HvADH1* and *HvADH2* have also been investigated. While *HvADH1* had some interesting activity, *HvADH2* had significantly better stability, unprecedented solvent tolerance, and broader substrate scope (Timpson et al. 2013). *HvADH2* soon became the benchmark for halophilic alcohol dehydrogenases with extensive further investigation into further enhancing its stability by covalent immobilization (Alsafadi and Paradisi 2014), mutagenesis to probe the active site and increase activity towards non-steroidal anti-inflammatory intermediates (Cassidy 2017) as well as its effective application in the asymmetric reduction of prochiral aromatic ketones (Alsafadi 2017). Two putative ADHs were then selected from the Red Sea and expressed in *Haloferax volcanii* using a stirred-tank bioreactor. This facilitated large-scale production and good yields of up to 17 mg gCDW⁻¹ of ADH/D1 (Strillinger et al. 2016).

The aim of this study was to mine the genome of *Haloquadratum walsbyi* to identify a novel ADH using *HvADH2* as a template for the search. Herein we describe the identification, heterologous expression, purification and characterisation of *HwADH*.

Results and discussion

Sequence alignment analysis

The genome of *Haloquadratum walsbyi* was sequenced and annotated over ten years ago (Bolhuis et al. 2006). Bio-product 3DM public alcohol dehydrogenase database was used to search for novel ADHs from *Haloquadratum walsbyi* (Kuipers et al. 2009). The sequence alignment across the ADH super-family was refined with keywords "*Haloquadratum walsbyi*" and four hits which were homologous to *HvADH2* from *Haloferax volcanii* (Fig. 1) were identified. Two hits were predicted to be an oxidoreductase (homolog to zinc containing alcohol dehydrogenase). One hit, "GOLGA5" had 65 % identity to *HvADH2* (Timpson et al. 2013).

FIG 1: 3DM dataset for Alcohol Dehydrogenase, a BLAST search with *HvADH2* as query sequence was performed and search was refined to "*Haloquadratum walsbyi*". *HwADH* corresponds to "GOLGA5".

Expression and purification of *HwADH*

The overexpression system in *Haloferax volcanii* was employed for the heterologous overexpression of *HwADH* (Allers et al. 2010). The gene *Hqrw_1156adh* was cloned into *pTA963* to generate a hexahistidine-tagged expression construct which was then transformed

into *Haloferax volcanii* strain, H1325. This strain features a double deletion of endogenous *adh1* and *adh2* and is our strain of choice for expression of ADHs. Expression of *HwADH* followed established protocols previously reported for *HvADH2* (Cassidy 2017). It is worth mentioning that *Hqrw_1156adh* was also cloned into pRSETb to probe expression in *E.coli*. Contrary to what reported for halorhodopsin, no expression (soluble or insoluble) was observed in *E. coli* for *HwADH* and this was not pursued further.

Expression of *HwADH* in *H. volcanii* was verified by activity assay with 10 mM BzOH in 3 M KCl, 50 mM Gly-KOH pH 10.0 buffer, the specific activity was 75.5 mU/mg. The protein was purified by immobilised Ni-affinity chromatography in one step. Stepwise elution with 2.5 mM and 10 mM followed by 50 mM EDTA resulted in 8 active fractions. Purified, homogenous fractions were pooled and dialyzed to remove EDTA. Notably, *HwADH* activity diminished following dialysis overnight. It was reasoned that the addition of ZnSO₄ (2 mM) into the dialysis buffer may prevent this loss in activity. It is postulated that the structural zinc in the protein plays an important stabilising role, and incubating the enzyme with Zn²⁺ allows recovery after purification in the presence of EDTA (Magonet et al. 1992). Indeed, when the purification was repeated and the enzyme dialysed in the presence of ZnSO₄, the specific activity reached a maximum of 650 mU/mg. The SDS-PAGE analysis of the purified *HwADH* is shown in Fig. 2, which revealed a band approximately corresponding to the subunit molecular weight of *HwADH* (36.2 kDa).

FIG 2: SDS-PAGE gel of *HwADH* IMAC purification in lanes 1-5, arrow depicts position of *HwADH* band (expected molecular weight 36.2 kDa), Lane 6: broad range protein marker Precision Plus Kaleidoscope, (10-250 kDa);

Expression levels between the halophilic ADHs characterised in our group varied strongly. The GC content of *Haloquadratum walsbyi* is low, 47.9 % and in comparison, *Haloferax volcanii* is 65 %. This could potentially affect codon recognition because the frequency of GC, specifically at the third position in the triplet, is only 41.63% for *Haloquadratum walsbyi* while its over 90% in *Haloferax volcanii*. However, pure *HwADH* (0.7 mg from one 300 mL culture) was obtained from expression in *Haloferax volcanii*, this is similar to *HmADH12* which yielded 2 mg of pure protein and was also expressed in *Hfx. volcanii* (Timpson et al. 2012).

Characterisation of *HwADH*

Purified *HwADH* showed a preference for KCl over NaCl, and exhibited the highest activity in buffers which featured 4 M KCl (Fig. 3). In terms of cofactor specificity, *HwADH* readily accepted NAD^+ and NADP^+ , with 10 mM BzOH and 1 mM cofactor, the specific activity was 600 mU/mg with NAD^+ and 580 mU/mg with NADP^+ . Hence, the enzyme displayed dual cofactor dependency. Enzyme kinetic experiments revealed that *HwADH* followed Michaelis-Menten kinetics with BzOH. Kinetic experiments with varied concentrations of BzOH and fixed cofactor (1 mM) confirmed that in the presence of BzOH, NADP^+ was the favoured cofactor over NAD^+ with K_m values of 0.8 mM and 2.0 mM respectively (Table 1). However, the calculated V_{\max} were virtually identical at 560 U/mg and 550 mU/mg, respectively. *HwADH* had a good affinity for BzOH in the presence of NADP^+ with a K_m is 2.5 times lower compared to NAD^+ .

FIG 3 *HwADH* salt dependence; Assay conditions: 10 mM BzOH, 1 mM NAD⁺ in 50 mM glycine buffer, pH 10.0.

Table 1: Kinetics of HwADH with varied concentrations of BzOH

	K_m (mM)	V_{max} (U/mg)
BzOH - NADP ⁺	0.8 ± 0.4	0.56 ± 0.05
BzOH - NAD ⁺	2.0 ± 0.7	0.55 ± 0.11

The remainder of assays were carried out with 10 mM BzOH, 1 mM NAD⁺ and 3 M KCl (to facilitate substrate solubility). The highest specific activity was observed at pH 10 in the oxidative reaction. *HwADH* is thermophilic, with an optimum temperature for oxidation of 65 °C (Fig. 4).

FIG 4 *HwADH* thermoactivity. Assay conditions: 10 mM BzOH, 1 mM NAD⁺ in 3 M KCl, 50 mM glycine buffer, pH 10.0.

HwADH displayed a preference for primary aromatic alcohol substrates, particularly with BzOH (657 mU/mg, Fig. 5). In comparison, activity with EtOH was approximately 10 times lower (65 mU/mg). Moderate activity was detected with the cyclic secondary alcohol, CycOH (150 mU/mg).

FIG 5 *HwADH* substrate specificity; substrate concentration was fixed at 10 mM for enantiopure substrates or 20 mM if racemic in 3 M KCl, 50 mM glycine buffer, pH 10.0 with 1 mM NAD⁺.

HwADH also accepted aromatic secondary alcohols such as 1-PheOH (76 mU/mg) and (*S*)-1-PheOH (30 mU/mg). (*R*)-1-PheOH was not a substrate for *HwADH*. Interestingly, 2-Phe-1-Prop was a good substrate (452 mU/mg) and when the enantiopure (*S*) and (*R*)-2-Phe-1-Prop were tested, it was observed that *HwADH* accepted both (165 mU/mg and 247 mU/mg respectively). This shows potential for *HwADH* to be applied to the dynamic kinetic resolution of arylpropanols (Galletti et al. 2010; Quaglia et al. 2013). Bulkier substrates were also accepted, *rac*-4-phenyl-2-butanol (72 mU/mg) and α -methyl-2-naphthalenemethanol (51 mU/mg); due to solubility, substrate concentrations were fixed at 2 mM in 3 M KCl, pH 10.0 and pH 6.0. *HwADH* catalyzed the reduction of aromatic ketones at pH 6.0 and pH 10.0 with 3 M KCl. Acetophenone was reduced at pH 10.0 (30 mU/mg) and phenylacetone was reduced at pH 6.0 (60 mU/mg) and pH 10.0 (40 mU/mg).

Solvent tolerance tests were performed with *HwADH* in the presence of 10 % (v/v) organic solvent (acetone, ACN, MeOH and iPrOH). *HwADH* standard activity tests were run with the addition of organic solvent (without pre-incubation) in 50 mM Gly-KOH buffer, pH 10 containing 3 M KCl at 50 °C. Methanol was the best co-solvent, *HwADH* retained 42 % activity compared to the control. Equally, in the presence of ACN and acetone, *HwADH* retained 37 and 39 %, respectively. *HwADH* was effected by iPrOH, retaining only 14 % activity. As a comparison, a similar study was performed with *HvADH2* with the same concentration of salt

and co-solvent (Alsafadi and Paradisi 2013). Under these conditions, the best solvent for *HvADH2* was also methanol, retaining over 40% activity. Notably, *HwADH* had higher activity in the presence of ACN (37%) compared to *HvADH2* (27%).

Experimental

Strain information of *Haloquadratum walsbyi*

The *Haloquadratum walsbyi* strain, DSM 16854, strain designation: C23 was purchased from DSMZ, Germany.

Cloning of *Hqrw_1156adh* into pTA963 and pRSETb

Primers *Hqrw_1156FWDNde* and *Hqrw_1156RVSBam* (Table 1) targeting the *Hwadh_1156* gene were designed based on the published nucleotide sequence (NCBI NC_017459.1) to include restriction sites for *NdeI* and *BamHI*, respectively. The *Hwadh_1156* gene was amplified in 50 µl reactions containing 0.5 µM of each primer, 200 µM dNTPs, 1 ng of genomic DNA, and 1 U of PhusionTM DNA polymerase in PhusionTM HF buffer (Finnzymes). Cycling conditions were a hot-start at 98 °C for 30 s, followed by 30 cycles of denaturation for 10 s at 98 °C, extension at 72 °C for 30 sec (annealing step was omitted as *T_m* of primers were greater than 72 °C). A final extension at 72 °C was employed for 10 min. NucleoSpin® Gel and PCR Clean-up (Macherey Nagel) kit was used for cleanup before the next step. The PCR product was treated with GoTaq® polymerase to facilitate A tailing for subcloning with the

StrataClone™ (Agilent) kit. Briefly, the reaction contained 4 µL PCR product (70 ng/µL), 2 µL 5x GoTaq Flexi reaction buffer, 1 µL dNTPs, 0.6 µL 25 mM MgCl₂, 1 µL GoTaq Flexi DNA polymerase and 1.4 µL sterile water. Reaction was incubated at 70 °C for 30 min. Without cleanup, adenylated DNA (2.5 µL) was incubated with cloning buffer (3 µL) and StrataClone vector mix (1 µL) for 30 min at room temp. Transformation into StrataClone SoloPack competent cells was performed as per manufacturer's instructions. Successful cloning was confirmed by bi-directional sequencing (MWG, Germany) using primers Hqwr_FWD_Seq and Hqwr_RVS_Seq (Table 2). To remove an internal NdeI site, a silent mutation (Table 1) was introduced into the *hwadh* gene harboured in the pSC-A plasmid using the QuikChange Lightning Multi Site-Directed Mutagenesis Kit provided by Agilent Technologies®.

The *Hwadh_1156* gene was then extracted from pSC and ligated into the *H. volcanii* vector pTA963 (provided by Dr. T. Allers) by a sequential restriction digest of pSC-A-hwadh and pTA963, respectively, using restriction enzymes NdeI and BamHI-HF (New England Biolabs, 1 U ml⁻¹) in their recommended buffers at 37°C overnight. Restriction products were visualized on a 0.8 % agarose gel containing ethidium bromide (0.5 µg ml⁻¹). Appropriate bands were excised and extracted using the Roche Agarose gel extraction Kit per manufacturer's instructions. Ligations (10 µl) were performed using molar insert-to-vector ratios of at least 2:1 and 1 U T4 DNA ligase (New England Biolabs) in the supplied buffer, at 16°C overnight. Nucleic acids from ligation were subjected to ethanol precipitation, electroporated into *E. coli* XL1-Blue® (Stratagene) ultracompetent cells and transformants were grown on LB agar and ampicillin. Positive colonies were inoculated into LB broth supplemented with ampicillin and grown overnight for plasmid extraction using the PureYield™ Plasmid Miniprep System (Promega) per manufacturer's instructions. Successful

cloning of pTA963-hwadh was confirmed by bi-directional sequencing (MWG, Eurofins) using primers Hqwr_FWD_Seq and Hqwr_RVS_Seq (Table 2).

Table 2: List of primers used in this study.

Primers	Sequence (5' → 3')
Hqrw_1156FWDNde	AAAA <u>CATATG</u> CACCACCACCACCACCACATGCGTGCTGCTGTTTA
Hqrw_1156RVSBam	GCGTCC <u>GGATCC</u> TTATATCTCAACAAGAACCTTAATTGCATCCCCG
Hqrw_115a891c	CAGTTCATCTGCATAGGCACGGACGGGAGCA
Hqwr_FWD_Seq	ACCTATTGCGCATATGCACCACCACCACCACCAC
Hqwr_RVS_Seq	CCGCTCTAGAACTAGTGGATCCGGGTGTGTCTTA

Primer sequences are presented in 5' → 3' format. Underlined regions are engineered restriction sites NdeI (CATATG) and BamHI (GGATCC) for the insertion into vector pTA963.

Complementary NdeI and BamHI restriction sites between *Hqrw_1156adh* and pRSETb facilitated the sub-cloning of *HwADH* directly from pTA963 available within the lab.

Expression and purification of *HwADH* in *Haloferax volcanii*

The transformation of pTA963-*Hwadh_1156* into H1325, production and purification of *HwADH* were performed as described previously (Timpson et al. 2012; Timpson et al. 2013).

A 1.1 g pellet was routinely recovered from a 300 mL culture and stepwise elution yielded 0.7 mg of pure protein. Purified *HwADH* was routinely stored at -20 °C. Protein concentrations were determined as previously described.

Enzyme assays

HwADH activity was determined by monitoring the production of the NAD(P)H cofactor at 340 nm, measured in intervals of 1 min for 20 min at 50 °C (Epoch 2 microplate reader, BioTek, Bad Friedrichshall, Germany; 96 Well Clear Flat Bottom UV-Transparent Microplate) (Corning®, 3635). All kinetic assays were performed in triplicate. The blank was treated adding the storage buffer (3 M KCl, 100 mM Tris-HCl, 2 mM ZnSO₄, pH 8.0 instead of enzyme.

Characterisation of HwADH

For the oxidative reaction, a range of Gly-KOH (pH 10.0) buffers based on KCl, ranging from 1 to 4 M were tested. The substrate specificity of *HwADH* was investigated by screening against a range of alcohol substrates (10 mM) EtOH, BzOH, 1-PheOH, (*S*)-1-PheOH, (*R*)-1-PheOH, 2-Phe-1-Prop, (*S*)-2-Phe-1-Prop and (*R*)-2-Phe-1-Prop. Ketone reduction was tested with 3 M KCl and citric acid-K₂PO₄ (pH 6.0) or Gly-KOH (pH 10.0) buffer, substrate concentration was 10 mM. The optimal temperature for *HwADH* was determined by screening activity between 30 and 65 °C, in the oxidative reaction. To investigate activity in the presence of organic

solvent, standard *HwADH* activity tests were performed with the addition of 10 % (v/v) organic solvents, acetone, acetonitrile (ACN), methanol (MeOH) and isopropanol (*i*-PrOH). Kinetics measurements were performed over a range of concentrations for BzOH (screened between 0 – 100 mM) in the presence of 1 mM NAD⁺ and 1 mM NADP⁺. Kinetic data were plotted using Prism 7 for Mac OS X with nonlinear regression analysis.

Conclusions

The aim of this study was to explore *Haloquadratum walsbyi* as a suitable additional source of novel halophilic alcohol dehydrogenases. A simple 3DM search and BLAST against our *HvADH2* from *Haloferax volcanii* identified a homologue which we named *HwADH*. *HwADH* from *Haloquadratum walsbyi* respected halophilic traits by requiring high salt concentrations for activity, was thermophilic, alkaliphilic and demonstrated some tolerance 10 % (v/v) organic solvents. *HwADH* exhibited dual cofactor specificity and accepted a broad range of substrates with a preference for primary aromatic alcohols and showed activity towards secondary aromatic substrates. There is potential to exploit the enzyme in the reduction of aromatic ketones. The heterologous expression in *Haloferax volcanii* facilitated the characterisation of *HwADH* but was low yielding compared to other halophilic enzymes. However, expression could be potentially improved by codon optimization for the host *Haloferax volcanii*. To the best of our knowledge, this is the first example of heterologous overexpression of a biocatalyst from *Haloquadratum walsbyi*.

Acknowledgments

The authors wish to acknowledge the support from the Synthesis and Solid State Pharmaceutical Centre and Science Foundation Ireland, Grant number 12/RC/2275, and Dr. Thorsten Allers for useful discussions.

References

- Allers T, Barak S, Liddell S, Wardell K, Mevarech M (2010) Improved strains and plasmid vectors for conditional overexpression of His-tagged proteins in *Haloferax volcanii*. Appl Environ Microbiol 76: 1759-1769
- Alsafadi D, Paradisi F (2013) Effect of organic solvents on the activity and stability of halophilic alcohol dehydrogenase (ADH2) from *Haloferax volcanii*. Extremophiles 17: 115-122
- Alsafadi D, Paradisi F (2014) Covalent immobilization of alcohol dehydrogenase (ADH2) from *Haloferax volcanii*: how to maximize activity and optimize performance of halophilic enzymes. Mol Biotechnol 56: 240-247
- Alsafadi D, Alsalman S, Paradisi F (2017) Extreme halophilic alcohol dehydrogenase mediated highly efficient syntheses of enantiopure aromatic alcohols. Org Biomol Chem 15: 9169-9175

- Becker EA et al. (2014) Phylogenetically driven sequencing of extremely halophilic archaea reveals strategies for static and dynamic osmo-response PLoS Genet 10(11), e1004784.
- Bolhuis H et al. (2006) The genome of the square archaeon *Haloquadratum walsbyi* : life at the limits of water activity. BMC Genomics 7: 169
- Borowitzka MA, Siva CJ (2007) The taxonomy of the genus *Dunaliella* (Chlorophyta, *Dunaliellales*) with emphasis on the marine and halophilic species. J Appl Phycol 19: 567-590
- Burns DG, Camakaris HM, Janssen PH, Dyll-Smith ML (2004) Cultivation of Walsby's square haloarchaeon. FEMS Microbiol Lett 238:469-473
- Cao Y, Liao L, Xu XW, Oren A, Wang C, Zhu XF, Wu M (2008) Characterization of alcohol dehydrogenase from the haloalkaliphilic archaeon *Natronomonas pharaonis*. Extremophiles 12:471-476
- Cassidy J, Bruen L, Rosini E, Molla G, Pollegioni L, Paradisi F (2017) Engineering substrate promiscuity in halophilic alcohol dehydrogenase (*HvADH2*) by in silico design. *PloS one*, 12(11), e0187482.
- Chellapandi P, Balachandramohan J (2011) Molecular evolution-directed approach for designing archaeal formyltetrahydrofolate ligase. Turk J Biochem 36:122-135
- Fu HY, Chang YN, Jheng MJ, Yang CS (2012) Ser(262) determines the chloride-dependent colour tuning of a new halorhodopsin from *Haloquadratum walsbyi*. Biosci Rep 32:501-509
- Galletti P, Emer E, Gucciardo G, Quintavalla A, Pori M, Giacomini D (2010) Chemoenzymatic synthesis of (2S)-2-arylpropanols through a dynamic kinetic resolution of 2-arylpropanals with alcohol dehydrogenases. Org Biomol Chem 8:4117-4123

- Hartman AL et al. (2010) The complete genome sequence of *Haloferax volcanii* DS2, a model archaeon. PLoS One 5:e9605
- Kuipers RK et al. (2009) Correlated mutation analyses on super-family alignments reveal functionally important residues. Proteins 76:608-616
- Large A, Stamme C, Lange C, Duan Z, Allers T, Soppa J, Lund PA (2007) Characterization of a tightly controlled promoter of the halophilic archaeon *Haloferax volcanii* and its use in the analysis of the essential cct1 gene. Mol Microbiol 66:1092-1106
- Liliensiek AK, Cassidy J, Gucciardo G, Whitely C, Paradisi F (2013) Heterologous overexpression, purification and characterisation of an alcohol dehydrogenase (ADH2) from *Halobacterium* sp. NRC-1. Mol Biotechnol 55:143-149
- Magonet E, Hayen P, Delforge D, Delaive E, Remacle J (1992) Importance of the structural zinc atom for the stability of yeast alcohol dehydrogenase. Biochem J 287:361-365
- Oren A (2002a) Halophilic microorganisms and their environments: (Vol. 5). Springer Science & Business Media.
- Oren A (2002b) Diversity of halophilic microorganisms: environments, phylogeny, physiology, and applications. J Ind Microbiol Biotechnol 28:56-63
- Quaglia D, Pori M, Galletti P, Emer E, Paradisi F, Giacomini D (2013) His-tagged Horse Liver Alcohol Dehydrogenase: Immobilization and application in the bio-based enantioselective synthesis of (S)-arylpropanols. Process Biochem 48:810-818
- Cuebas-Irizarry MF, Irizarry-Caro RA, López-Morales C, Badillo-Rivera KM, Rodríguez-Minguela CM, Montalvo-Rodríguez R (2017) Cloning and Molecular Characterization of an Alpha-Glucosidase (MalH) from the Halophilic Archaeon Haloquadratum walsbyi Life 7:46

- Sellek GA, Chaudhuri JB (1999) Biocatalysis in organic media using enzymes from extremophiles. *Enzyme Microb Technol* 25:471-482
- Stoeckenius W (1981) Walsby's square bacterium: fine structure of an orthogonal procaryote. *J Bacteriol* 148:352-360
- Strillinger E, Grötzinger SW, Allers T, Eppinger J, Weuster-Botz D (2016) Production of halophilic proteins using *Haloferax volcanii* H1895 in a stirred-tank bioreactor. *Appl Microbiol Biotechnol* 100:1183-1195
- Sudo Y et al. (2011) A microbial rhodopsin with a unique retinal composition shows both sensory rhodopsin II and bacteriorhodopsin-like properties. *J Biol Chem* 286:5967-5976
- Timpson LM, Alsafadi D, Mac Donnchadha C, Liddell S, Sharkey MA, Paradisi F (2012) Characterization of alcohol dehydrogenase (ADH12) from *Haloarcula marismortui*, an extreme halophile from the Dead Sea. *Extremophiles* 16:57-66
- Timpson LM et al. (2013) A comparison of two novel alcohol dehydrogenase enzymes (ADH1 and ADH2) from the extreme halophile *Haloferax volcanii*. *Appl Microbiol Biotechnol* 97:195-203
- Walsby AE (1980) A square bacterium. *Nature* 283:69-71
- Yu HY, Li X (2014) Characterization of an organic solvent-tolerant thermostable glucoamylase from a halophilic isolate, *Halolactibacillus* sp. SK71 and its application in raw starch hydrolysis for bioethanol production. *Biotechnol Prog* 30:1262-1268

FIG 1

Search: Haloquadratum walsbyi							
#	Accession	Subfamily	Description	Species	Identities	E-value	Coverage
45	U1ML29	2DPHB (CI 0.31)	Threonine dehydrogenase related Zn-dependent dehydrogenase	Haloquadratum walsbyi J07HQP1	221/348 (64%)	2.7e-155	<div><div></div></div> Export hit to insert
46	U1NG79	2DPHB (CI 0.32)	Threonine dehydrogenase related Zn-dependent dehydrogenase	Haloquadratum walsbyi J07HQP2	218/348 (63%)	9.6e-155	<div><div></div></div> Export hit to insert
47	Q18DS9	2DPHB (CI 0.32)	Oxidoreductase (Homolog to zinc-containing alcohol dehydrogenase)	Haloquadratum walsbyi (strain DSM 16790 / HBSQ001)	222/348 (64%)	3.9e-153	<div><div></div></div> Export hit to insert
48	G0LGA5	2DPHB (CI 0.32)	Oxidoreductase (Homolog to zinc-containing alcohol dehydrogenase)	Haloquadratum walsbyi (strain DSM 16854 / JCM 12705 / C23)	221/348 (64%)	4.8e-153	<div><div></div></div> Export hit to insert

Showing 1 to 4 of 4 entries (filtered from 100 total entries)

FIG 2

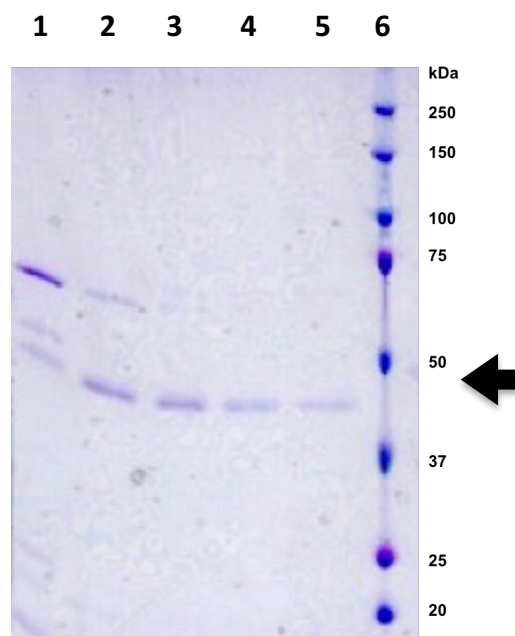


FIG. 3

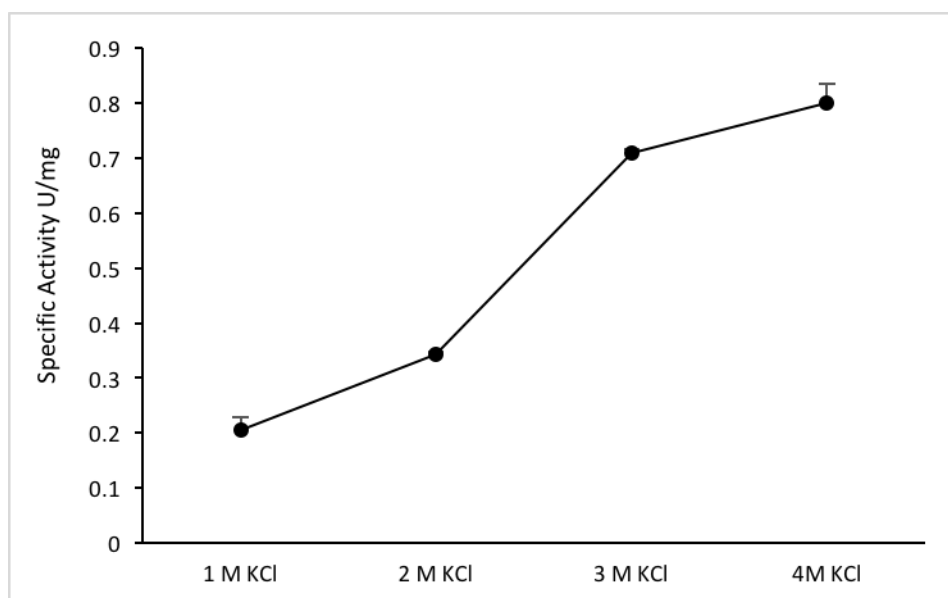


FIG 4

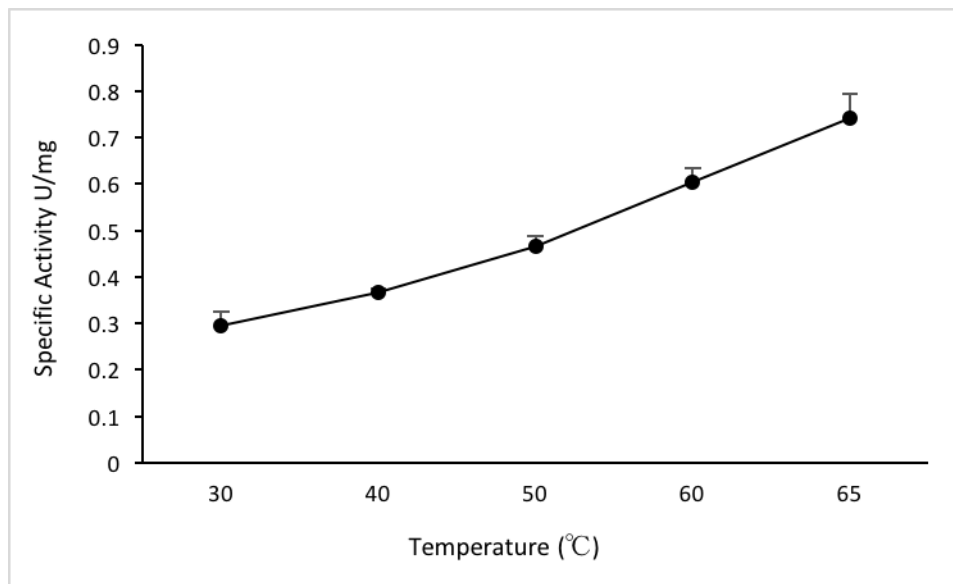


FIG 5

